# LPV $\mathcal{H}_2$ State Feedback Controller for Automated Parking System

Ju Won Seo, *Graduate Student Member, IEEE*, Dae Jung Kim, *Graduate Student Member, IEEE*, Jin Sung Kim, *Graduate Student Member, IEEE*, and Chung Choo Chung, *Member, IEEE*

***Abstract*—In this letter, we propose a linear parameter-varying (LPV) kinematic model for automated parking systems. We also design an LPV $\mathcal{H}_2$ state feedback controller with the proposed model. The vehicle kinematic model is intrinsically a nonlinear system, but we show that the kinematic model can be represented as an LPV kinematic model. The state feedback control gain is obtained using convex interpolation in the $\mathcal{H}_2$ sense of a linear matrix inequality approach. We will show that the proposed parking system guarantees the stability of the closed-loop system with disturbances. To validate the proposed method, we conduct parking experiments with a test vehicle for two scenarios. Using the proposed LPV $\mathcal{H}_2$ state feedback controller, the vehicle tracks paths for all scenarios, reaching the final parking spot and showing smooth steering performance. The results show that the lateral position error and the heading angle error are smaller than 0.05 m and 0.005 rad, respectively.**

***Index Terms*—Autonomous vehicles, linear parameter-varying systems.**

## I. Introduction

In THE automated parking system (APS) field, it is common to use both path planning and control algorithms. Path planning finds a trajectory the vehicle can follow from a starting position to a goal position while avoiding obstacles or driving in a narrow space. State-of-the-art approaches for path planning are reported in [1]. Given a vehicle path to track, the APS can apply classic feedback control methods that make the system robust to its model uncertainties, disturbances, and sensor noises. Many parking control researches use nonlinear control [2], predictive control [3], and sliding-mode control [4]. However, using only a feedback control has a trade–off between the transient response performance and the control input. Thus, feedforward control is mostly used with feedback control for APSs [5]. In summary, smooth path planning, steering, and tracking performance should be considered in the sense of vehicle control.

The vehicle kinematic model is commonly used for vehicle control in APSs. It is well known that the vehicle kinematic model is based purely on geometric relationships governing the system, while the vehicle dynamic model considers the forces that affect the motion [6]. Because the vehicle kinematic model is derived under the assumption that there is no tire slip angle, it is reliable when each wheel's velocity vector is in the wheel's direction. This is a reason that the vehicle kinematic model has been used for the limited low speed [7]–[9]. Therefore, the vehicle kinematic model needs fewer vehicle parameters than the vehicle dynamic model, including some unknown or uncertain vehicle parameters such as cornering stiffness and the vehicle's inertia [9]. For this reason, it was recently reported that there are several types of research that apply the kinematic model to the autonomous driving field, such as the lane-keeping system (LKS) [10], path planning [11], and lane estimation [12].

The vehicle kinematic model is intrinsically a nonlinear system. Therefore, when we utilize the kinematic model, some problems exist, such as nonlinearity in the kinematic model or an assumption of constant vehicle speed. It could be challenging to control the vehicle due to model mismatch and uncertainty. Therefore, it needs to consider the vehicle's varying speed and convert a nonlinear model into a time-varying linear model. In this case, the linear model with varying parameters can be utilized as a linear parameter-varying (LPV) framework [10]. In the framework, we can design the robust controller in consideration of model uncertainty as varying parameter [13]. Therefore, the LPV method might be useful in the parking problem with the kinematic model. However, new LPV modeling for the APS is needed since the LPV model used in [10] is for highway driving.

This letter proposes an LPV kinematic model for lateral motion control and an LPV $\mathcal{H}_2$ state feedback controller for the automated parking system. The LPV kinematic model consists of time-varying parameters with velocity and a newly defined parameter. The nonlinear model can be converted to

Manuscript received March 4, 2021; revised May 6, 2021; accepted May 12, 2021. Date of publication May 26, 2021; date of current version June 28, 2021. This work was supported by the National Research Foundation of Korea (NRF) Grant funded by the Ministry of Science and ICT (MSIT, Data-Driven Optimized Autonomous Driving Technology Using Open Set Classification Method) under Grant 2021R1A2C2009908. Recommended by Senior Editor C. Seatzu. *(Corresponding author: Chung Choo Chung.)*

Ju Won Seo, Dae Jung Kim, and Jin Sung Kim are with the Department of Electrical Engineeing, Hanyang University, Seoul 04763, South Korea (e-mail: suhju1227@hanyang.ac.kr; dandyj88@hanyang.ac.kr; jskim06@hanyang.ac.kr).

Chung Choo Chung is with the Division of Electrical and Biomedical Engineering, Hanyang University, Seoul 04763, South Korea (e-mail: cchung@hanyang.ac.kr).

Digital Object Identifier 10.1109/LCSYS.2021.3083977

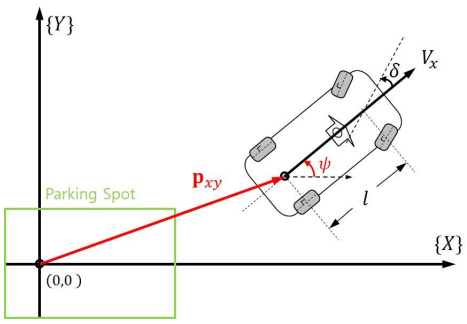


Fig. 1. Parking coordinates and nonholonomic vehicle model at the center of the rear axle (*cra*) of the vehicle.

the discrete time-varying linear model. We show that no matter where the initial point is, there exists a convex interpolation of the time-varying parameters during the parking motion. Then, we design the LPV $\mathcal{H}_2$ state feedback controller with feedforward control based on the kinematic motion, which is made with a predefined path. The optimal control gain is obtained at three vertices in the $\mathcal{H}_2$ sense of a linear matrix inequality (LMI). Then, the gain scheduling is designed using convex interpolation with the optimal control gain such that the sub-optimal gain is obtained in the convex set. In the sequel, the proposed parking system guarantees the stability of the closed-loop system with disturbances. To verify the performance of the proposed LPV $\mathcal{H}_2$ state feedback controller, parking experiments for two scenarios are conducted with a test vehicle. The experiments' results show that the state feedback controller compensates for model uncertainty which the feedforward controller does not consider. The vehicle tracks the path to reach the parking spot and observes the smooth steering performance. Further, the results show that the lateral position error and the heading angle error are smaller than 0.05 m and 0.005 rad, respectively.

## II. Vehicle Kinematic Model and Path Planning

This section develops a lateral kinematic model and describes a clothoid path for an automated parking system.

### A. Vehicle Kinematic Model

To begin with, let us consider the parking coordinates $\{XY\}$, as shown in Fig. 1. We define the vehicle position vector $\mathbf{p}_{xy} = \begin{bmatrix} X & Y \end{bmatrix}^T \in \mathbb{R}^2$ at the center of the rear axle (*cra*) in the parking coordinates. With the orientation $\psi$ of the vehicle at the *cra*, the vehicle pose $\mathbf{p}_{cra} \in \mathbb{R}^3$ is defined by

$$\mathbf{p}_{cra} = \begin{bmatrix} \mathbf{p}_{xy} \\ \psi \end{bmatrix} = \begin{bmatrix} X \\ Y \\ \psi \end{bmatrix}. \tag{1}$$

This letter assumes the Ackerman turning geometry and the bicycle model [9]. Further, the vehicle slip angle is neglected. We use a discrete-time kinematic model, and the process of converting from a continuous-time kinematic model is derived in [5], [14]. Using a zero-order hold with sampling rate $T_s$, we then have the vehicle kinematic model in the form of

$$X(k+1) = X(k) + T_s V_x(k) \cos(\psi(k)) \tag{2a}$$

$$Y(k+1) = Y(k) + T_s V_x(k) \sin(\psi(k))$$

$$\psi(k+1) = \psi(k) + T_s \frac{V_x(k)}{l} \tan(\delta(k)). \tag{2b}$$

where $V_x(\cdot)$, $\delta(\cdot)$, and $l$ are the longitudinal velocity at the *cra*, the front wheel steering angle, and the wheelbase, respectively. Note that (2) is divided into the longitudinal motion model (2a) and the lateral motion model (2b) for the decentralized controller [14].

*Remark 1:* The longitudinal velocity is obtained through the desired velocity design by $V_x^d(k) = -\nu X(k)$ for any $\nu \in (0, 2/T_s)$ [14] and a simple feedback control law, e.g., PD control, to track the desired velocity, considering a simplified model of the power train dynamics given by $\ddot{x}(k+1) = (1 - \frac{T_s}{\tau})\ddot{x}(k) + \frac{T_s}{\tau}\ddot{x}^d(k)$ with a time constant $\tau$ [9]. Further, we limit $|V_x^d(\cdot)|$ to take into account the vehicle kinematic motion for parking operation. The details of the vehicle's longitudinal motion are beyond the scope of this work.

In this letter, we focus on lateral motion control considering the time-varying velocity. In addition, to take into account a nonlinear characteristics due to the orientation $\psi$, we define a state dependent parameter $\varsigma(\cdot)$, which is a *Sinc function* of $\psi(\cdot)$, such as

$$\varsigma(\cdot) = \begin{cases} 1 & \text{for } \psi(\cdot) = 0, \\ \frac{\sin\psi(\cdot)}{\psi(\cdot)} & \text{otherwise.} \end{cases} \tag{3}$$

Let us consider the state $\mathbf{x} = \begin{bmatrix} Y & \psi \end{bmatrix}^T$ for lateral motion control, the control input $u = \tan^{-1}(\delta)$, and the unknown but bounded disturbance $\mathbf{w} = \begin{bmatrix} w_1 & w_2 \end{bmatrix}^T$. Then, from (2b) and (3) we can obtain a discrete time-varying linear system, representing a vehicle kinematic lateral motion model in the form of

$$\mathbf{x}(k+1) = \Phi(\mathbf{x}(k))\mathbf{x}(k) + \Gamma(k)u(k) + \Gamma_w \mathbf{w}(k) \tag{4}$$

where

$$\Phi(\mathbf{x}(k)) = \begin{bmatrix} 1 & T_s V_x(k)\varsigma(\mathbf{x}(k)) \\ 0 & 1 \end{bmatrix},$$

$$\Gamma(k) = \begin{bmatrix} 0 \\ V_x(k)\frac{T_s}{l} \end{bmatrix}, \quad \Gamma_w(k) = \begin{bmatrix} \gamma_{w,11} & 0 \\ 0 & \gamma_{w,22} \end{bmatrix}.$$

Here, $\Gamma_w$ represents the disturbance matrix as a design factor for the $\mathcal{H}_2$ state feedback controller. Note that $V_x(\cdot)$ is limited with a desired low speed, a negative value in the proposed parking coordinates for reverse parking, and $\varsigma(\cdot)$ is bounded in the range of $[\frac{2}{\pi}, 1]$ with an assumption that the vehicle's orientation moves in $-\frac{\pi}{2} \le \psi(\cdot) \le \frac{\pi}{2}$. This orientation range is appropriate for the automated parking system.

### B. Clothoid Path Model

Every path should have a slow varying continuous curve to ensure that vehicles can track it considering the vehicle motion control. To this end, a clothoid is defined as a spiral whose curvature is a linear function of its arc length. The overall path we design is shown in Fig. 2. The parking spot $\mathbf{p}_1$ is the origin of the parking coordinates as well as the origin of the path. A clothoid path is made as a transition from $\mathbf{p}_0$ to $\mathbf{p}_1$, taking a radius $R_0$ of a circle tangent to the vehicle's $x$-axis at the *cra* at the initial pose of the vehicle. Given the arc length $s$ of a

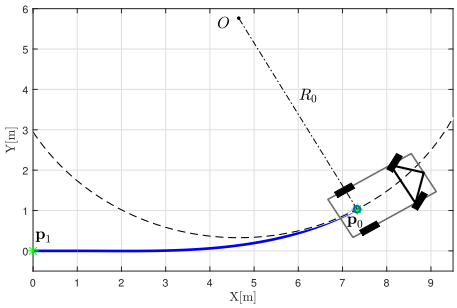


Fig. 2. Path planning using a clothoid path.

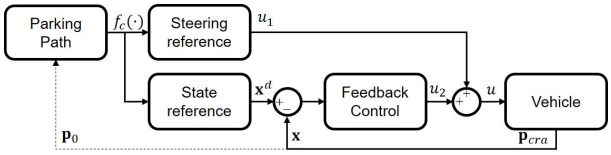


Fig. 3. The overall structure of the parking lateral control system.

path, the slowly varying curvature can be designed with the clothoid path construction rule as follows:

$$\kappa(s) = 2c_2 + 6c_3 s \tag{5}$$

where $c_2$ and $c_3$ denote the path curvature at $s = 0$ and its variation rate, respectively. The tangent angle $\varphi(s)$, at the arc length, is obtained as the integral of the curvature (5) by

$$\varphi(s) = c_1 + 2c_2 s + 3c_3 s^2 \tag{6}$$

where $c_1$ is the initial tangent angle at $s = 0$. Then, parametric expressions for the proposed parking coordinates are represented by [15]

$$\begin{aligned} X(s) &= X_1 + \int_0^s \cos(c_1 + 2c_2\sigma + 3c_3\sigma^2)d\sigma \\ Y(s) &= Y_1 + \int_0^s \sin(c_1 + 2c_2\sigma + 3c_3\sigma^2)d\sigma \end{aligned} \tag{7}$$

where $X_1$ and $Y_1$ are the initial longitudinal and lateral position of the clothoid path at $s = 0$, respectively. Note that $Y_1$ and $c_1$ are zeros, and $X_1$ is a design factor for a straight line since the parking's objective is to move the vehicle to be aligned with the parking spot. Then, our control purpose is to track and regulate this path.

## III. Vehicle Motion Control

In this letter, for the simplicity of analysis, there is no obstacle considered in path planning. In fact, we implicitly consider that the automated parking system is embedded in a hierarchical architecture in which a higher-level planner solves the obstacle avoidance problem and provides a series of motion goals to the lower control layer. In that context, given space free of obstacles, we use both a feedforward controller and a feedback controller. Figure 3 represents the overall structure of the lateral control system for automated parking. It is well known that feedback control makes the system robust, and feedforward control improves transient response performance [5]. To this end, we design the control input $u = u_1 + u_2$ where $u_1$ is the feedforward controller to track the desired path and $u_2$ is the state feedback controller based on the LPV $\mathcal{H}_2$ performance to compensate for model uncertainties and disturbances.

### A. Feedforward Control

Under the steady-state condition with an assumption of a constant velocity, we see that

$$\dot{\psi} = \frac{V_x}{R} = \frac{V_x}{l}\tan(\delta) \tag{8}$$

where $R$ is the radius of a circle tangent to the vehicle's $x$-axis at the *cra* (see details in Fig. 1). From (8), it is immediate to design the desired steering angle as

$$\delta_{ff} = \tan^{-1}\left(\frac{l}{R}\right) = \tan^{-1}(\kappa l) \tag{9}$$

where $1/R = \kappa$ [9]. Substituting (5) into (9), the desired steering angle can be presented as follows:

$$\delta_{ff} = \tan^{-1}(2c_2 l + 6c_3 s l),$$

then, with $u_1 := \tan^{-1}(\delta_{ff})$ the feedforward controller is obtained as

$$u_1 = 2c_2 l + 6c_3 s l.$$

Furthermore, we can derive the desired state $\mathbf{x}^d = \begin{bmatrix} Y^d & \psi^d \end{bmatrix}^T$ from equation (6) and its integration [12] as follows:

$$\begin{aligned} Y^d(s) &= c_1 s + c_2 s^2 + c_3 s^3, \\ \psi^d(s) &= c_1 + 2c_2 s + 3c_3 s^2. \end{aligned} \tag{10}$$

In this letter, we consider $Y^d(0) = 0$ to align the vehicle with the parking spot. The vehicle can be controlled with only the feedforward controller under the assumptions that the velocity is constant and there is no model uncertainty, disturbance, and noise. If these assumptions are not satisfied, the parking performance is not guaranteed, and we need a feedback compensator. To cope with this problem, in the next subsection, we will show how to design the LPV $\mathcal{H}_2$ state feedback controller to make the system robust against such uncertainties.

### B. LPV $\mathcal{H}_2$ State Feedback Controller Design and Performance Analysis

The longitudinal velocity $V_x(\cdot)$ and heading angle $\psi(\cdot)$ are varying but bounded. Therefore, let us define the varying parameter $\boldsymbol{\theta} \in \mathbb{R}^2$ by

$$\boldsymbol{\theta} = [\theta_1 \;\; \theta_2]^T = [V_x\varsigma \;\; V_x]^T.$$

To design the state feedback controller $u_2$, the LPV lateal motion model of (4) is obtained with the varying parameter $\boldsymbol{\theta}$ as follows:

$$\mathbf{x}(k+1) = \Phi(\boldsymbol{\theta})\mathbf{x}(k) + \Gamma(\boldsymbol{\theta})u_2(k) + \Gamma_w\mathbf{w}(k) \tag{11}$$

where

$$\Phi(\boldsymbol{\theta}) = \begin{bmatrix} 1 & T_s\theta_1 \\ 0 & 1 \end{bmatrix}, \Gamma(\boldsymbol{\theta}) = \begin{bmatrix} 0 \\ \frac{T_s}{l}\theta_2 \end{bmatrix}.$$

Note that $\theta_1$ and $\theta_2$ are bounded because the vehicle velocity $V_x$ is limited, and $\varsigma$ is bounded. Therefore, we can obtain

boundaries of the varying parameters by

$$\theta_1 \in [\underline{\theta}_1 \quad \bar{\theta}_1],\ \theta_2 \in [\underline{\theta}_2 \quad \bar{\theta}_2]. \tag{12}$$

Given the parameter vector $\boldsymbol{\theta}$, it can be represented in the polytopic form by

$$\boldsymbol{\theta} = \mathbf{V}\boldsymbol{\xi} \tag{13}$$

where $\boldsymbol{\xi} \in \mathbb{R}^3$ denotes the convex interpolation parameter vector satisfying $\xi_i \geq 0$ for $i = 1, 2, 3$, $\sum_{i=1}^{3} \xi_i = 1$ and $\mathbf{V} \in \mathbb{R}^{2\times 3}$ presents the vertex matrix. Here, $|\theta_1| \leq |\theta_2|$ is always satisfied due to $\varsigma(\cdot) \leq 1$, so the region of varying parameter $\boldsymbol{\theta}$ is made tighter than the region using four vertexes. Further, no matter where the initial point is chosen, $\boldsymbol{\theta}$ becomes an interior point of the convex set made by the vertexes during the parking motion. Therefore, we design the vertex matrix $\mathbf{V}$ as follows:

$$\mathbf{V} = \begin{bmatrix} \underline{\theta}_1 & \bar{\theta}_1 & \bar{\theta}_1 \\ \underline{\theta}_2 & \bar{\theta}_2 & \underline{\theta}_2 \end{bmatrix}. \tag{14}$$

The vertex matrix $\mathbf{V}$ should be invertible for the convex interpolation parameter vector $\boldsymbol{\xi}$ to be uniquely determined by the given varying parameter vector $\boldsymbol{\theta}$. To this end, we define an augmented matrix $\bar{\mathbf{V}}$ by

$$\bar{\mathbf{V}} = \begin{bmatrix} \mathbf{V} \\ \mathbf{1}_{1\times 3} \end{bmatrix} = \begin{bmatrix} \underline{\theta}_1 & \bar{\theta}_1 & \bar{\theta}_1 \\ \underline{\theta}_2 & \bar{\theta}_2 & \underline{\theta}_2 \\ 1 & 1 & 1 \end{bmatrix}. \tag{15}$$

Then, $\boldsymbol{\xi}$ is uniquely obtained by $\boldsymbol{\xi} = \bar{\mathbf{V}}^{-1}[\boldsymbol{\theta}^T \quad 1]^T$. Given the convex interpolation parameter $\xi_i$ for $i = 1, 2, 3$, parameter-dependent $\Phi(\boldsymbol{\theta})$ and $\Gamma(\boldsymbol{\theta})$ is then composed of

$$\begin{aligned} \Phi(\boldsymbol{\theta}) &= \sum_{i=1}^{3} \xi_i \Phi^{(i)} \\ \Gamma(\boldsymbol{\theta}) &= \sum_{i=1}^{3} \xi_i \Gamma^{(i)} \end{aligned} \tag{16}$$

where

$$\begin{aligned} &\Phi^{(1)} = \Phi(\underline{\theta}_1),\ \Phi^{(2)} = \Phi(\bar{\theta}_1),\ \Phi^{(3)} = \Phi(\bar{\theta}_1) \\ &\Gamma^{(1)} = \Gamma(\underline{\theta}_2),\ \Gamma^{(2)} = \Gamma(\bar{\theta}_2),\ \Gamma^{(3)} = \Gamma(\underline{\theta}_2). \end{aligned}$$

Then, we can have the system matrix pairs $G^{(i)}$ as follows:

$$G^{(i)} \coloneqq [\Phi^{(i)} \mid \Gamma^{(i)}] \tag{17}$$

for $i = 1, 2, 3$. Considering (16), we see that (11) can be represented as a multi input multi output (MIMO) system such as in Fig. 4 in the form of

$$P(\boldsymbol{\theta}) : \begin{cases} \mathbf{x}(k+1) = \Phi(\boldsymbol{\theta})\mathbf{x}(k) + \Gamma(\boldsymbol{\theta})u_2(k) + \Gamma_w \mathbf{w}(k) \\ \mathbf{z}(k) = C_1\mathbf{x}(k) + D_{12}u_2(k) \\ \mathbf{y}(k) = C_2\mathbf{x}(k) \end{cases} \tag{18}$$

where $\mathbf{z} \in \mathbb{R}^2$ is the objective function signal including the state and control input combination,

$$\begin{aligned} &C_2 = I_{2\times 2},\ D_{11} = 0_{3\times 2},\ D_{21} = 0_{2\times 2},\ D_{22} = 0_{2\times 1}, \\ &C_1 = \begin{bmatrix} c_{11} & 0 \\ 0 & c_{22} \\ 0 & 0 \end{bmatrix},\ \text{and } D_{12} = \begin{bmatrix} 0 \\ 0 \\ d_{31} \end{bmatrix}. \end{aligned}$$

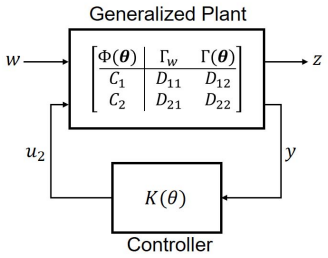


Fig. 4. Generalized plant of the system.

Note that for $V_x(\cdot) \neq 0$, the generalized MIMO system (18) satisfies the following considerations for the optimal control design.

- The system matrices $(\Phi^{(i)}, \Gamma^{(i)})$ are stabilizable for each given vertex index $i$ for $i = 1, 2, 3$.
- The pairs $(\Phi^{(i)}, C_1)$ have no unobservable modes on the imaginary axis.
- $D_{12}^T D_{12}$ is invertible.
- $D_{12}^T C_1 = 0$.

To guarantee the closed-loop system's stability and $\mathcal{H}_2$ performance, we design the LPV $\mathcal{H}_2$ state feedback controller $K(\theta)$. Using $u_2(k) = K(\boldsymbol{\theta})\mathbf{x}(k)$, the closed-loop system in the state-space form is given by

$$\mathcal{T}_{zw} : \begin{cases} \mathbf{x}(k+1) = (\Phi(\boldsymbol{\theta}) + \Gamma(\boldsymbol{\theta})K(\boldsymbol{\theta}))\mathbf{x}(k) + \Gamma_w w(k) \\ \mathbf{z}(k) = (C_1 + D_{12}K(\boldsymbol{\theta}))\mathbf{x}(k). \end{cases} \tag{19}$$

*Theorem 1 (Robust Stability and $\mathcal{H}_2$ Performance):* Given a set

$$\Omega \coloneqq \{G(\boldsymbol{\theta}) \mid G(\boldsymbol{\theta}) = \sum_{i=1}^{3} \xi_i G^{(i)}, \xi_i \geq 0, \sum_{i=1}^{3} \xi_i = 1\},$$

consider the closed-loop discrete-time LPV system (19). If there exists two symmetric matrices $W^{(i)} \in \mathbb{R}^{3\times 3} > 0$, $P \in \mathbb{R}^{2\times 2} > 0$ and $Z^{(i)} \in \mathbb{R}^{1\times 2}$ for a given $\gamma > 0$ such that

$$\begin{aligned} tr(W^{(i)}) &< \gamma^2, \\ \begin{bmatrix} W^{(i)} & C_1 P + D_{12}Z^{(i)} \\ * & P \end{bmatrix} &> 0, \\ \begin{bmatrix} P & \Phi^{(i)}P + \Gamma^{(i)}Z^{(i)} & \Gamma_w \\ * & P & 0 \\ * & * & I \end{bmatrix} &> 0, \end{aligned} \tag{20}$$

then the closed-loop system (19) is parametrically dependent stabilizable by the state feedback $K(\theta) = \sum_{i=1}^{3} \xi_i K^{(i)}$ with $K^{(i)} = Z^{(i)}P^{-1}$. Moreover, $K(\theta)$ is also guaranteed for $\mathcal{H}_2$ performance, as $\|\mathcal{T}_{zw}\|_2^2 < \gamma^2$ for all $\{\Phi(\boldsymbol{\theta}), \Gamma(\boldsymbol{\theta})\} \in \Omega$ [16].

*Proof:* With the change of variable $Z^{(i)} = K^{(i)}P$, applying Schur complement to

$$\begin{bmatrix} P & \Phi^{(i)}P + \Gamma^{(i)}Z^{(i)} & \Gamma_w \\ * & P & 0 \\ * & * & I \end{bmatrix} > 0, \tag{21}$$

leads to the Lyapunov inequality as follows:

$$\hat{\Phi}^{(i)} P \hat{\Phi}^{(i)T} - P + \Gamma_w \Gamma_w^T < 0 \tag{22}$$

where $\hat{\Phi}^{(i)} = \Phi^{(i)} + \Gamma^{(i)}K^{(i)}$. For the closed-loop LPV system (19), if there exists a positive-definite matrix $P$,

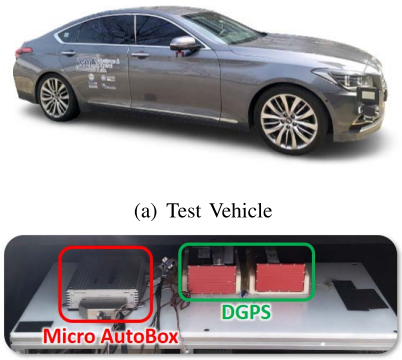

(a) Test Vehicle




(b) Control System

Fig. 5. Experimental vehicle and control system (a) Test Vehicle, (b) Control System.

then (22) presents that the closed-loop system is stabilizable. To guarantee the $\mathcal{H}_2$ performance, the constraint is given by

$$trace((C_1 + D_{12}K^{(i)})P(C_1 + D_{12}K^{(i)})^T) < \gamma^2. \quad (23)$$

Applying the Schur complement to (23) leads to the following constraints:

$$\begin{bmatrix} W^{(i)} & C_1P + D_{12}Z^{(i)} \\ * & P \end{bmatrix} > 0$$
$$tr(W^{(i)}) < \gamma^2. \quad (24)$$

Hence, the linear matrix inequality (LMI) conditions, (21) and (24), originate from the parameter-dependent Lyapunov inequality and the $\mathcal{H}_2$ constraints. It can be shown that LMIs for each vertex using $\Omega$ in (20) can be transformed into (21) and (24). ■

By solving LMI equation (20), each state feedback control gain is calculated as $K^{(i)} = Z^{(i)}P^{-1}$ of each vertex. Then, the LPV $\mathcal{H}_2$ state feedback controller can be obtained by

$$K(\boldsymbol{\theta}) = \sum_{i=1}^{3} \xi_i K^{(i)}. \quad (25)$$

## IV. Experimental Results

The plant to be controlled consisted of a luxury sedan, the Genesis G80 from Hyundai Motors with an in-vehicle sensor, a differential global positioning system (DGPS), and a control system as shown in Fig. 5. The in-vehicle sensor was used to measure the steering wheel angle and the longitudinal vehicle speed. Further, the DGPS was mounted on the *cra* of the test vehicle. The vehicle pose was measured in the parking coordinates. The control algorithm was implemented in a Micro-Autobox from dSPACE. The AutoBox was installed and logged data from each sensor using the Controller Area Network (CAN) bus. The vehicle's variable longitudinal speed was used from 0 km/h to −5 km/h during experiments since a human driver manually controlled the vehicle.

The proposed method considered the longitudinal speed and orientation angle for varying parameters. As soon as the DGPS and in-vehicle sensors obtain the controller design parameters,

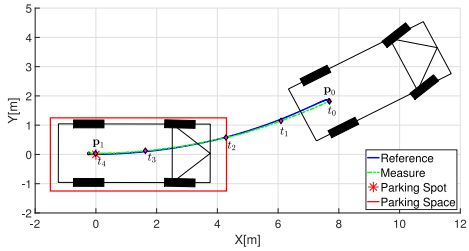


(a) Vehicle Pose $\mathbf{p}_{xy}$ at the Parking Coordinates

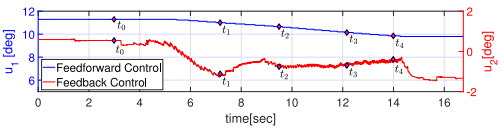


(b) Feedforward Control $u_1$ and Feedback Control $u_2$

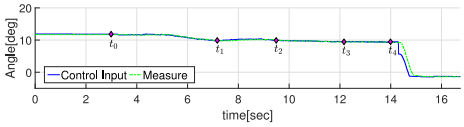


(c) Control Input $u$

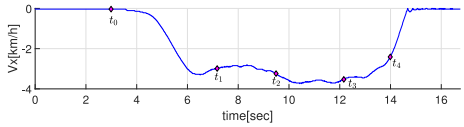


(d) Longitudinal Speed $V_x$

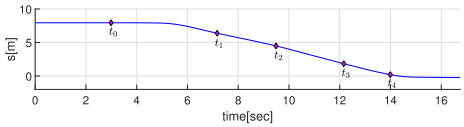


(e) Arc Length $s$

Fig. 6. Scenaio 1: (a) Vehicle Pose $\mathbf{p}_{xy}$ at the Parking Coordinates, (b) Feedforward Control $u_1$ and Feedback Control $u_2$, (c) Control Input $u$ (d) Longitudinal Speed $V_x$, (e) Arc Length $s$.

the parking system starts to move the vehicle. If the longitudinal speed is near zero, then the system is weakly controllable so that the control gain becomes excessively large. Therefore, we limit the longitudinal speed such as $|V_x| \geq 0.1m/s$ in designing the control gain. To establish the proposed LPV $\mathcal{H}_2$ performance, we experimented with two test scenarios with different initial vehicle poses and steering angles.

1) Scenario 1: $\mathbf{p}_0 = \begin{bmatrix} 7.6890 & 1.8090 & 0.4779 \end{bmatrix}^T$
2) Scenario 2: $\mathbf{p}_0 = \begin{bmatrix} 7.6330 & -1.6140 & -0.4498 \end{bmatrix}^T$

We first generated a clothoid path from $\mathbf{p}_0$ to $\mathbf{p}_1$ as shown in Fig. 2. The purpose of the experiment is to track the generated clothoid path and accurately reach the parking spot. We commonly used $c_{11} = \sqrt{10}$, $c_{22} = \sqrt{2}$ and $d_{31} = 1$ for the robust controller. In two scenarios, Figs. 6 (a) and 7 (a) show that the vehicle tracks the generated clothoid path well to reach parking spot $\mathbf{p}_1$. Further, Figs. 6 (b) and 7 (b) show the feedforward control input $u_1$ and the feedback control input $u_2$. Figures 6 (c) and 7 (c) also show control input $u = u_1 + u_2$ and a measured value for each scenario. The measured value was calculated from the steering wheel angle. There is a difference between the control input and the measurement due to the steering dynamics of the vehicle. In addition, the longitudinal

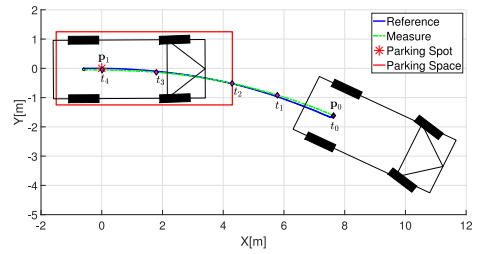


(a) Vehicle Pose $\mathbf{p}_{xy}$ at the Parking Coordinates

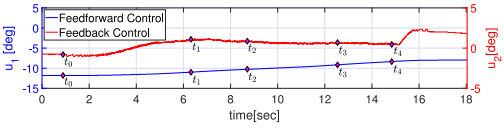


(b) Feedforward Control $u_1$ and Feedback Control $u_2$

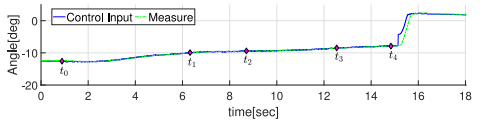


(c) Control Input $u$

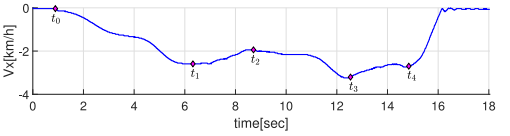


(d) Longitudinal Speed $V_x$

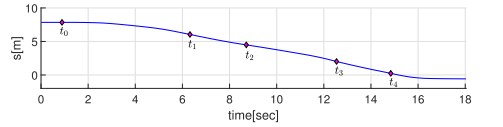


(e) Arc Length $s$

Fig. 7. Scenario 2: (a) Vehicle Pose $\mathbf{p}_{xy}$ at the Parking Coordinates, (b) Feedforward Control $u_1$ and Feedback Control $u_2$, (c) Control Input $u$ (d) Longitudinal Speed $V_x$, (e) Arc Length $s$.

speed for each scenario is shown in Figs. 6 (d) and 7 (d), and Figs. 6 (e) and 7 (e) show the arc length of the path connecting the parking spot and the position of the current vehicle over time. The experiment results show that the vehicle speed is not constant because the human driver used his foot to manually control the longitudinal speed, which leads to the arrival at the rear, passing the parking spot. That is why the final arc length is smaller than 0. However, this letter focuses on lateral control, for which we have seen the proposed method's parking performance. Some model uncertainties include varying variables depending on the vehicle velocity, which can be generated by tire deformation, the steering system, and slip during vehicle movements. The experiments' results show that the state feedback controller compensates for model uncertainty which the feedforward controller does not consider. The vehicle tracks the path to reach the parking spot and observes the smooth steering performance. Moreover, we obtained the results of $|\mathbf{x}^d - \mathbf{x}| \leq \begin{bmatrix}0.05 & 0.005\end{bmatrix}^T$ at the final parking spot $\mathbf{p}_1$ in both scenarios. A video clip can be seen at `https://youtu.be/ORS3N9uHCkg` in which Case 2, Case 3 are Scenario 1 and, Scenario 2, respectively.

## V. Conclusion

This letter proposed the LPV kinematic model for lateral motion control and the LPV $\mathcal{H}_2$ state feedback controller for automated parking systems. The LPV kinematic model consisted of time-varying parameters with varying velocity and the newly defined state-dependent parameter so that the nonlinear model is converted to linear kinematics. We then designed the LPV $\mathcal{H}_2$ state feedback controller with the feedforward control based on the kinematic motion as the given path. The control gain was obtained using convex interpolation in the $\mathcal{H}_2$ sense using the LMI approach. We observed that the proposed parking system guarantees the closed-loop system's stability with disturbances. The proposed method performed two parking scenarios with a test vehicle. The vehicle tracked the path well and observed the smooth steering performance in all scenarios. The errors of the two states' reference values and measurement values at the final parking spot were smaller than 0.05 m and 0.005 rad, respectively.

## References

[1] D. González, J. Pérez, V. Milanés, and F. Nashashibi, "A review of motion planning techniques for automated vehicles," *IEEE Trans. Intell. Transp. Syst.*, vol. 17, no. 4, pp. 1135–1145, Apr. 2016.

[2] A. Ohata and M. Mio, "Parking control based on nonlinear trajectory control for low speed vehicles," in *Proc. Int. Conf. Ind. Electron. Control Instrum.*, 1991, pp. 107–112.

[3] T. Tashiro, "Vehicle steering control with MPC for target trajectory tracking of autonomous reverse parking," in *Proc. IEEE Int. Conf. Control Appl.*, 2013, pp. 247–251.

[4] X. Du and K. K. Tan, "Autonomous reverse parking system based on robust path generation and improved sliding mode control," *IEEE Trans. Intell. Transp. Syst.*, vol. 16, no. 3, pp. 1225–1237, Jun. 2015.

[5] A. D. Luca, G. Oriolo, and C. Samson, "Feedback control of a nonholonomic car-like robot," in *Robot Motion Planning and Control*. Heidelberg, Germany: Springer, 1988, pp. 171–253.

[6] C. M. Kang, H.-H. Lee, and C. C. Chung, "Comparative evaluation of dynamic and kinematic vehicle models," in *Proc. 53rd IEEE Conf. Decis. Control*, Dec. 2014, pp. 648–653.

[7] G. Indiveri, "Kinematic time-invariant control of a 2D nonholonomic vehicle," in *Proc. 38th IEEE Conf. Decis. Control*, Dec. 1999, pp. 2112–2117.

[8] K. Lee, D. Kim, W. Chung, H. W. Chang, and P. Yoon, "Car parking control using a trajectory tracking controller," in *Proc. SICE-ICASE Int. Joint Conf.*, 2006, pp. 2058–2063.

[9] R. Rajamani, *Vehicle Dynamics and Control*. Heidelberg, Germany: Springer, 2011.

[10] C. M. Kang, S.-H. Lee, and C. C. Chung, "Linear parameter varying design for lateral control using kinematics of vehicle motion," in *Proc. Annu. Amer. Control Conf.*, 2018, pp. 3239–3244.

[11] P. Polack, F. Altche, B. d'Andrea Novel, and A. de La Fortelle, "The kinematic bicycle model: A consistent model for planning feasible trajectories for autonomous vehicles?" in *Proc. IEEE Int. Veh. Symp.*, Jun. 2017, pp. 812–818.

[12] C. Kang, S.-H. Lee, and C. C. Chung, "Multirate lane-keeping system with kinematic vehicle model," *IEEE Trans. Veh. Technol.*, vol. 67, no. 10, pp. 9211–9222, Oct. 2018.

[13] S. Skogestad and I. Postlethwaite, *Multivariable Feedback Control: Analysis and Design*. Hoboken, NJ, USA: Wiley, 2007.

[14] D. J. Kim and C. Chung, "Automated perpendicular parking system with approximated clothoid-based local path planning," *IEEE Control Syst. Lett.*, vol. 5, no. 6, pp. 1940–1945, Dec. 2021.

[15] M. Brezak and I. Petrović, "Path smoothing using clothoids for differential drive mobile robots," in *Proc. 18th IFAC World Congr.*, Aug. 2011, pp. 1133–1138.

[16] K. Zhou and J. C. Doyle, *Essentials of Robust Control*, vol. 104. Upper Saddle River, NJ, USA: Prentice-Hall, 1998.